Chemistry of Metals and Alloys

Chem. Met. Alloys 2 (2009) 18-24
Ivan Franko National University of Lviv
www.chemetal-journal.org

Crystal structure, electron structure and physical properties of RM_5Si_3 compounds, R = Y, Gd, Tb, Dy, Ho, Er, Tm, Yb, Lu; M = Ni, Co

Yu. GORELENKO[1]*, R. MATVIISHYN[1], I. SHCHERBA[1,2], V. PAVLYUK[1], R. SERKIZ[3]

[1] *Ivan Franko National University of Lviv, Kyryla i Mefodiya St. 6, 79005 Lviv, Ukraine*
[2] *Institute of Techniques, Academy of Pedagogy, Podchorazych St. 2, 30-084 Krakow, Poland*
[3] *Scientific Technical and Educational Center of Low Temperature Studies, Dragomanov St. 50, 79005 Lviv, Ukraine*
* *Corresponding author. E-mail: gorelenko_yuriy@franko.lviv.ua*

Received December 3, 2008; accepted June 26, 2009; available on-line November 16, 2009

RM_5Si_3 intermetallic compounds (R = a heavy rare earth metal or yttrium, M = Ni or Co) were synthesized by arc melting. X-ray phase and structure analyses were used to determine the composition of the samples. The crystal structure was refined for some of the compounds and the elemental composition of the compounds was confirmed by scanning electron microscopy. X-ray emission spectral studies of the Si $K\beta_{1,x}$, Si $L_{II,III}$, M $K\beta_{2,5}$, and M $L\alpha$-lines were used to establish the valence band structure, and electrical and magnetic properties were investigated.

Crystal structure / Intermetallic compounds / X-ray spectra / Electric properties / Magnetic susceptibility

Introduction

Rare earth – transition metal – silicon (R–M–Si) intermetallic compounds are interesting as materials for the construction of nuclear fuel reactors. Their relatively high heat resistance and high neutron absorption cross-section make them promising for the use as neutron capture materials. The investigation of possible applications of these compounds in radio engineering, electronics, computing technology, etc., is in progress. The electric conduction, thermoionic, and magnetic properties are being investigated as well [1].

The first RCo_5Si_3 compound was found in the Y–Co–Si ternary system [2]. Several isostructural RCo_5Si_3 (R = Dy, Ho, Er, Tm, Lu) intermetallic compounds with the UCo_5Si_3 structure type [3] were reported short time later. The crystal structure of the RNi_5Si_3 compounds, where R = Y, Gd, Tb, Ho, Er, Tm, Yb, was investigated in [4]; $DyNi_5Si_3$ and $LuNi_5Si_3$ were also found to crystallize with YNi_5Si_3-type structures [5].

Experimental

The samples were synthesized from rare earth metals (the main metal content was 99.9 wt.%), carbonyl iron (Fe content 99.99 wt.%), electrolytic nickel (N0 brand, 99.99 wt.%), cobalt (K0 brand, 99.99 wt.% Co), and silicon ("semiconducting brand", Si content better than 99.999 wt.%) by arc melting the constituents with a non-consumable tungsten electrode on a water-cooled copper hearth under a protective atmosphere of high-purity Ti-gettered argon. The mass loss of the initial charges did not exceed 0.5 wt.%. The ingots were annealed in evacuated (0.1 Pa) silica ampoules at 1070 K for 800 h. The microstructure was studied using an optical metallographic microscope (magnification ×200÷300). The elemental composition of some samples was confirmed using a registering scanning electron microscope REMMA–102–02.

X-ray patterns of all the alloys were taken at room temperature on an X-ray DRON-2.0M powder diffractometer with Fe $K\alpha$ radiation ($\theta/2\theta$ scan, $30^o \le 2\theta \le 150^o$), using pure silicon as an internal standard. The magnetic susceptibility (χ) was measured by the Faraday method in fields up to 0.8 MA/m in the temperature range 83÷1150 K. The temperature dependence of the resistivity (ρ) at 78÷400 K was measured by a two-probe technique on rectangular specimens cut by a spark erosion machine in cold water. The differential thermopower (S) with respect to pure copper was measured in the temperature range 78÷380 K.

Table 1 Lattice parameters and magnetic characteristics of RNi_5Si_3 and RCo_5Si_3 compounds.

Compound	$a(\Delta a)$, Å	$b(\Delta b)$, Å	$c(\Delta c)$, Å	μ_{eff}, μ_B	Θ_p, K
YNi_5Si_3	18.62(2)	3.779(5)	6.706(2)	–	–
$GdNi_5Si_3$	18.72(2)	3.808(3)	6.634(8)	7.99(4)	-22(2)
$TbNi_5Si_3$	18.63(3)	3.789(3)	6.639(9)	9.73(5)	-8(2)
$DyNi_5Si_3$	18.67(8)	3.790(1)	6.634(3)	10.69(5)	-27(5)
$HoNi_5Si_3$	18.61(1)	3.784(4)	6.626(6)	10.63(5)	-2(5)
$ErNi_5Si_3$	18.59(1)	3.764(3)	6.620(6)	9.56(7)	-24(1)
$TmNi_5Si_3$	18.52(4)	3.753(1)	6.744(8)	7.61(5)	-13(8)
$YbNi_5Si_3$	18.53(1)	3.744(3)	6.610(6)	4.55(4)	-38(1)
$LuNi_5Si_3$	18.49(2)	3.739(3)	6.710(2)	–	–
YCo_5Si_3	14.858(9)	–	3.730(5)	–	–
$DyCo_5Si_3$	14.884(5)	–	3.687(1)	10.77(6)	17.2(8)
$HoCo_5Si_3$	14.883(2)	–	3.6805(7)	10.66(9)	-9.8(9)
$ErCo_5Si_3$	14.843(1)	–	3.664(1)	9.67(5)	-7.6(6)
$TmCo_5Si_3$	14.844(2)	–	3.670(1)	7.7(1)	-5.7(2)
$LuCo_5Si_3$	14.822(2)	–	3.652(1)	–	–

Table 2 Experimental and crystallographic data for $ErCo_5Si_3$.

Compound	$ErCo_5Si_3$	
Structure type	UCo_5Si_3	
Space group	$P6_3/m$	
Pearson symbol	$hP54$	
Lattice parameters, Å	a = 14.8837(1), b = 14.8837(1), c = 3.6848(1)	
Absorption coefficient, mm^{-1}	35.386	
Theta range for data collection	from 4.18° to 25.34°	
Limiting indices	$-17 \le h \le 17$; $-17 \le k \le 17$; $-4 \le l \le 4$	
Reflections collected/unique	504/477	
Refinement method	full-matrix least-squares on F^2	
Data / restraints / parameters	504/0/57	
Goodness-of-fit on F^2	0.518	
Final R indices [$I > 2\text{sigma}(I)$]	$R1$ = 0.0208, $wR2$ = 0.0492	
R indices (all data)	$R1$ = 0.0194, $wR2$ = 0.0473	
Extinction coefficient	0.0019(1)	
Residual electron density, e·Å^{-3}	1.103 and -2.140	
Atomic coordinates and displacement parameters:	$x\ y\ z$, $U_{11}\ U_{22}\ U_{33}\ U_{12}\ U_{13}\ U_{23}$ (Å^2)	
Er (6*h*)	0.39692(3) 0.10078(3) 1/4	0.0059(2) 0.0054(2) 0.0058(2) 0.00318(17) 0 0
Co1 (6*h*)	0.65188(9) 0.22505(9) 1/4	0.0042(6) 0.0039(6) 0.0070(6) 0.0023(5) 0 0
Co2 (6*h*)	0.45958(9) 0.92548(9) 1/4	0.0037(6) 0.0039(6) 0.0070(6) 0.0017(5) 0 0
Co3 (6*h*)	0.27177(9) 0.22127(9) 1/4	0.0043(6) 0.0038(6) 0.0066(6) 0.0018(5) 0 0
Co4 (6*h*)	0.14900(9) 0.41627(9) 1/4	0.0038(6) 0.0044(6) 0.0069(6) 0.0022(5) 0 0
Co5 (6*h*)	0.14344(17) 0.02845(11) 1/4	0.0778(14) 0.0052(7) 0.0062(7) 0.0145(8) 0 0
Si1 (6*h*)	0.44258(18) 0.76094(18) 1/4	0.0035(11) 0.0028(11) 0.0028(11) 0.0029(9) 0 0
Si2 (6*h*)	0.13628(18) 0.25482(18) 1/4	0.0025(11) 0.0035(11) 0.0059(12) 0.0005(9) 0 0
Si3 (6*h*)	0.43197(18) 0.37083(18) 1/4	0.0045(11) 0.0038(11) 0.0059(12) 0.0019(9) 0 0

Single crystals, suitable for X-ray analysis, of the $ErCo_5Si_3$ compound were investigated by the Laue and Weissenberg methods (RKV-86 and RGNS-2 chambers, Mo $K\alpha$ radiation), and then mounted on an automatic single-crystal diffractometer Xcalibur3^{TM} CCD (Mo $K\alpha$ radiation, graphite monochromator, ω-scans). The data collection and reduction were performed with CrysAlis CCD [6] and CrysAlis RED [7] programs. The crystal structure was solved and refined using the SHELXL-97 [8] program package and the crystallographic data were standardized with the program Structure Tidy [9]. Experimental and crystallographic data are given in Tables 1 and 2. The K-emission Co (or Ni) and Si spectra for the RNi_5Si_3 and RCo_5Si_3 compounds were taken with a DRS-@M X-ray spectrometer. Quartz crystals (10-10 and 13-40), radius of curvature 0.5 m, were used as crystal analyzer. The apparatus distortion was equal to 0.3 eV for the Co (Ni) $K\beta_{2,5}$- and Si $K\beta$-spectra, respectively. The $M\ L\alpha$-spectrum was measured with the same spectrometer, using a mica crystal (001) as crystal analyzer.

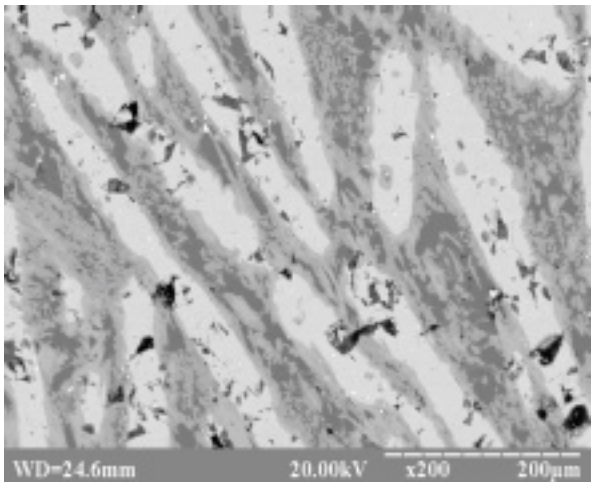

Phase colour	Elemental composition
Grey (main)	$DyCo_5Si_3$
Dark grey	$DyCo_9Si_4$
Clear	$DyCo_2Si_2$

Fig. 1 EDAX image of the $Dy_{11.12}Co_{55.55}Si_{33.33}$ alloy.

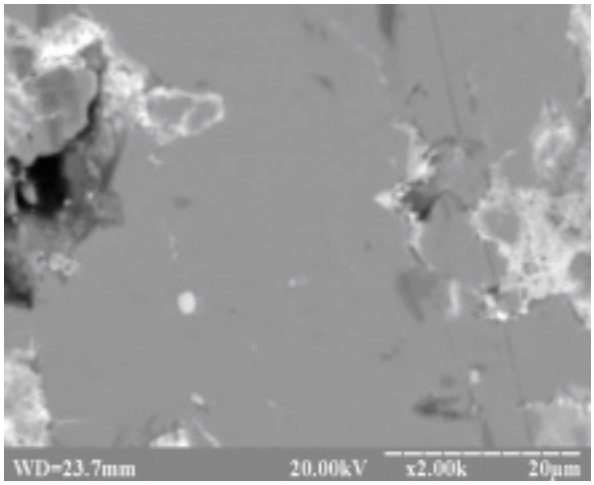

Phase colour	Elemental composition
Grey (main)	$DyNi_5Si_3$

Fig. 2 EDAX image of the $Dy_{11.11}Ni_{55.55}Si_{33.33}$ alloy.

Results and discussion

The crystal structures of the RNi_5Si_3 and RCo_5Si_3 compounds belong to the YNi_5Si_3 type (space group *Pnma*) and UCo_5Si_3 type (space group $P6_3/m$), respectively. Images of the metallographic sections are shown in Figs. 1-5. To obtain reliable interatomic distances, we determined the lattice and atomic parameters by X-ray powder diffraction for $DyNi_5Si_3$ and $HoCo_5Si_3$. The atomic parameters of the crystal structure of the $HoCo_5Si_3$ compound were refined from 108 reflections, using the CSD program package [10]. All the atoms occupy positions 6(*h*): *x y* ¼: Ho – (*x* = 0.4038(6), *y* = 0.1068(6), B_{iso} = 1.19 Å^2); Co(1) – (0.652(2), 0.240(1), 1.07); Co(2) – (0.459(2), 0.930(2), 0.37); Co(3) – (0.274(2), 0.233(1), 0.04); Co(4) – (0.162(1), 0.412(1), 1.64); Co(5) – (0.152(2), 0.018(1), 1.86); Si(1) – (0.430(3), 0.742(3), 1.26); Si(2) – (0.149(2), 0.251(2), 0.21); Si(3) – (0.425(3), 0.361(3), 0.74), respectively. The *R*-factor was 0.1311. The lattice parameters are: *a* = 14.883(5) and *c* = 3.680(4) Å.

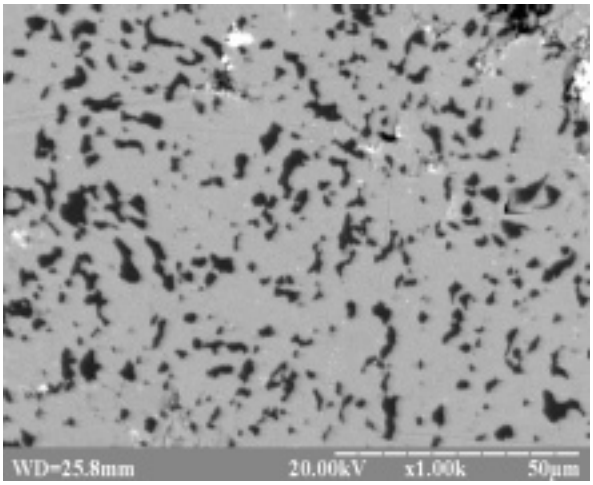

Phase colour	Elemental composition
Grey (main)	$ErCo_5Si_3$

Fig. 3 EDAX image of the $Er_{11.11}Co_{55.55}Si_{33.33}$ alloy.

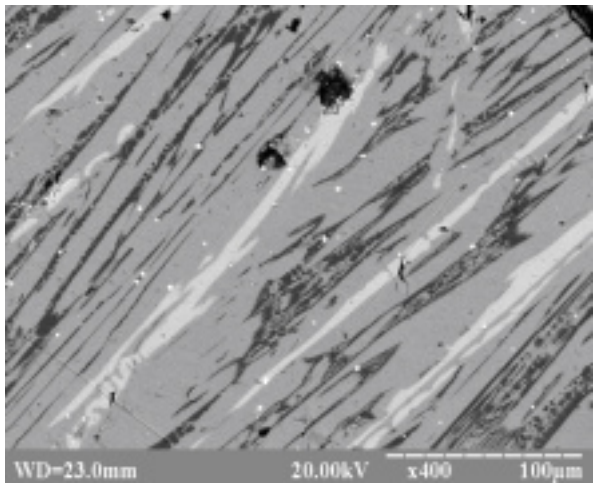

Phase colour	Elemental composition
Grey (main)	$ErNi_5Si_3$
Clear	$ErNi_2Si_2$

Fig. 4 EDAX image of the $Er_{11.11}Ni_{55.55}Si_{33.33}$ alloy.

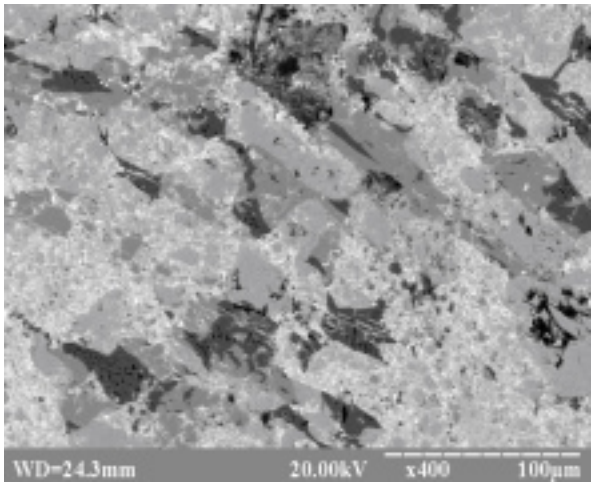

Phase colour	Elemental composition
Grey (main)	$TmCo_5Si_3$
Clear	$TmCo_2Si_2$

Fig. 5 EDAX image of the $Tm_{11.11}Co_{55.55}Si_{33.33}$ alloy.

The atomic parameters of the $DyNi_5Si_3$ compound were determined from 60 observed and 30 "zero" (i.e. the intensities were insignificant) diffracted reflections, using the CSD program package. The atoms occupy positions 4(*c*): *x* ¼ *z*: Dy – (*x* = 0.142(1), *z* = 0.882(4), B_{iso} = 1.00 Å^2); Ni(1) – (0.292(3), 0.673(7), 1.04); Ni(2) – (0.497(5), 0.359(7), 2.52); Ni(3) – (0.008(4), 0.633(6), 0.14); Ni(4) – (0.112(3), 0.364(7), 2.63); Ni(5) – (0.298(3), 0.070(6), 0.09); Si(1) – (0.419(7), 0.099(6), 0.30); Si(2) – (0.236(6), 0.383(8), 1.54); Si(3) – (0.413(6), 0.635(9), 0.88), respectively. The *R*-factor was 0.089. The lattice parameters are: *a* = 18.67(8), *b* = 3.790(1), and *c* = 6.634(3) Å.

Infinite "propeller" prism columns exist in both structures; the coordination polyhedra (CP) of the silicon atoms have composition Ho_2Co_4 or Dy_2Ni_4. The CPs of the Ho and Dy atoms are 20-vertex polyhedra, which are similar in the two structures. The CPs of the Ni and Co atoms are mainly distorted cubes with additional atoms above the faces.

The mean value of the δ_{Co-Si} distances in $HoCo_5Si_3$ is 2.340 Å, that is near 3.5% less than the sum r_{Co} + r_{Si}, whereas the mean value of the δ_{Co-Co} distances, 2.565 Å, is by 2.4% larger than $2r_{Co}$. It is worth noting that the structure contains isolated triangles formed by Co atoms, the distances between which are reduced by 10.4% with respect to $2r_{Co}$.

The mean value of the interatomic distances δ_{Ni-Si} in $DyNi_5Si_3$ is 2.38 Å, which is 1.6% less than the sum (r_{Ni} + r_{Si}) (where r_{Si}, the radius of the Si atom, is 1.173 Å). The mean values of the δ_{Ni-Ni} distances in the CPs of the Ni atoms are increased within the range 2.8–10% as compared with $2r_{Ni}$. The mean value is 2.67 Å, which is by 7.2% higher than the theoretical value of $2r_{Ni}$.

There are no direct contacts between nickel atoms in the $DyNi_5Si_3$ structure. However, isolated triangles of silicon atoms with δ_{Si-Si} = 2.271 Å exist, which gives evidence for strong "metallization" of the Si atoms in these structures (for comparison, $2r_{Si}$ = 2.346 Å).

Based on these data, one can assume the existence of a certain covalent component in the bonds between Ni and Si atoms, as well as between Co and Si atoms, and the decrease of the exchange interaction between the Ni atoms and partially between the Co atoms. X-ray spectra of Ni and Si in the RNi_5Si_3 (*R* = Y, Gd, Tb, Dy) compounds, on a common energy scale, are shown in Fig. 6.

The fine structure of the silicon spectra is considerably richer than for the nickel spectra and is particularly sensitive to changes in the nearest neighborhood. Unlike the spectra of pure silicon where the (*p* + *s*) band, with different contributions of some symmetries, occupies the whole width of the filled part of the valence band, the distribution is considerably changed in the RNi_5Si_3 compounds. The presence of only metal atoms in the trigonal prisms, which are the principal feature of the CP of Si, results in strong localization of electronic states of *p*- and *s*-symmetry of the emitting atom.

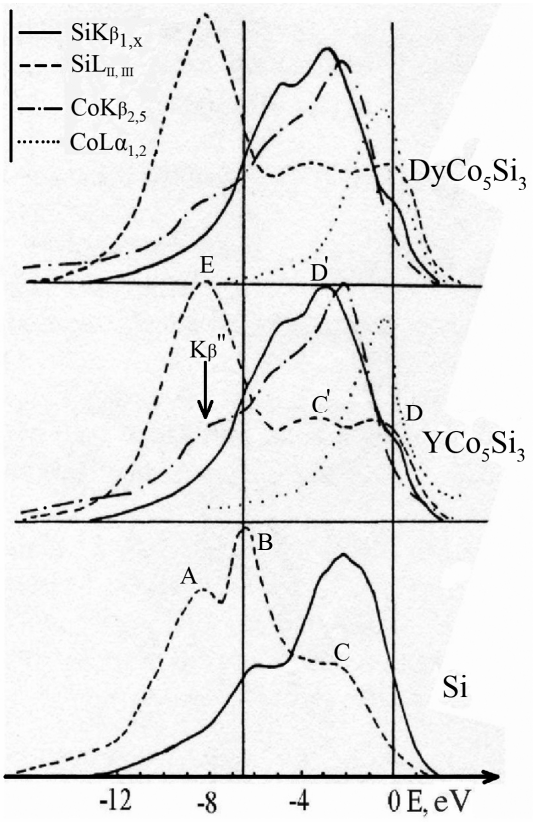

Fig. 6 The spectra of the RNi_5Si_3 (*R* = Y, Gd, Tb, Dy) compounds shown on a unified energy scale (full line Si $K\beta_{1,x}$, dashed line Si $L_{II,III}$, dash-dotted line Ni $K\beta_{2,5}$, dotted line Ni $L\alpha_{1,2}$).

The differences between the crystallographically distinct Si atoms are insignificant, and can thus not have any direct effect on the energy of the valence states. A detailed examination of the X-ray parameters of the Si $K\beta_{1,x}$ band shows that, in comparison with the corresponding band of pure Si, the maximum *D*, which represents the density of *p*-states of Si, is shifted towards the low-energy side by approximately 2 eV and practically coincides with the maximum *H* of the Si $L_{II,III}$ band (Fig. 6). Such a shift of the maximum in the distribution of the electronic density of Si *p*-symmetry can be explained by a small transfer of Si negative charge into unfilled *d*-levels of nickel. Besides, the reduction of the symmetry index of the Ni $L\alpha_{1,2}$ line, as a result of the lowering of the non-compensated spin density on the Ni atoms, indicates also an increase of the number of Ni *d*-electrons, which, finally, leads to paramagnetism in the RNi_5Si_3 intermetallics.

The appearance of the high energy maximum *K*, the intensity of which is somewhat lower in comparison with the $R_2Ni_3Si_5$ compounds [11], indicates a considerable hybridization of *p*- and *d*-wave functions of Si and Ni, respectively. The reduced Ni–Si distances as compared with the sum (r_{Ni} + r_{Si}) are an indication in the same sense. The presentation of the spectra on a common energy scale shows that in the majority of the intermetallic silicides [12-14], the $L\alpha$-band of Ni practically coincides with the maxima *K* and *A* of the fine structure of the Si *p*- and *s*-bands, respectively (Fig. 6). Thus, the maximum of the $L\alpha$-band of nickel diminished in the high-energy part of the valence band. It should be noted that there is no complete match of the high-energy maxima *K* and *A* with the $L\alpha$-band. However, we can state that conditions for *p*-*d* resonance (which take place in the RCu_2Si_2 compounds [13]) do not show up in the YNi_5Si_3 structure. The ratio of the intensities of the maxima *A* and *C* can serve as criterion for the assessment of the contribution of the Ni *d*-state to the $L_{II,III}$-band of Si when quantum-mechanical calculations are absent. The increase of the number of Ni atoms surrounding the Si atoms from 3 in $R_2Ni_3Si_5$ to 7 in RNi_5Si_3 leads to an increase of the I_A/I_C ratio, which indicates a considerably larger contribution of the Ni *d*-states in the sub-Fermi region in the RNi_5Si_3 compounds than in the $R_2Ni_3Si_5$ compounds.

The $K\beta_{2,5}$-band of Ni occupies almost all the valence bands in the RNi_5Si_3 compounds. The maximum *C* is somewhat shifted to the middle of the valence band as compared with the $L\alpha$-band of pure Ni, which results in a decrease of the overlapping integral of the wave functions of *p*- and *d*-symmetries. Another important characteristic pointing toward the existence of Ni–Si bonds is the presence of a $K\beta``$- satellite (Fig. 6), the formation of which hybridized *s*-states of Si substantially contribute to. Together with the localization of *p*-states of silicon, its *s*-states also have a tendency to narrowing, which is demonstrated by the single local maximum *C* in the spectrum. Thus, the 4*p*-states of nickel and the 3*s*-states of silicon are in the lowest energy position and form the bottom of the valence band.

The general behavior described above for the X-ray spectra of nickel and silicon in the RNi_5Si_3 compounds applies to the RCo_5Si_3 compounds as well (Fig. 7).

The presence of the $K\beta``$-satellite on the Co $K\beta_{2,5}$-band makes it possible to show the silicon and cobalt spectra on a common scale of energies, which considerably improves their self-descriptive. The structure of the Si $K\beta_{1,x}$-band has a distinctly outlined three-band shape for all the compounds. The appearance of the high-energy maximum of the $K\beta_{1,x}$-band and its match with the main maximum of the Co $L\alpha$-band show the existence of hybridization of *d*-states of Co and *p*-states of Si (Fig. 7). Thus, the top of the valence band of the compounds studied here is formed by *d*-states of Co, part of which are hybridized with *s*- and *p*-states of silicon. It is necessary to note that, because of the shift of the maximum of the *d*-states in the high-energy region, the wave functions of the Co *p*- and *d*-electrons overlap less in these compounds than in pure Co.

The highest density of *p*-states of Co and Si is observed in the middle part of the valence band, where the density of *p*-states of Si decreases by approximately a factor of two, and *d*-states of Co are almost completely absent. Electrons of this sub-band can partially form bonds of the covalent type between Co and Si atoms, an interpretation which is supported by the considerable overlapping of their *p*-functions and the presence of short Co–Si distances.

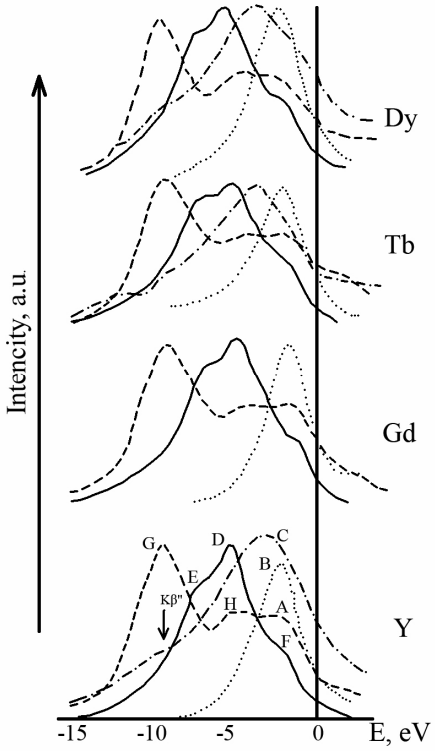

Fig. 7 The spectra of the RCo_5Si_3 (*R* = Y, Dy) compounds shown on a unified energy scale.

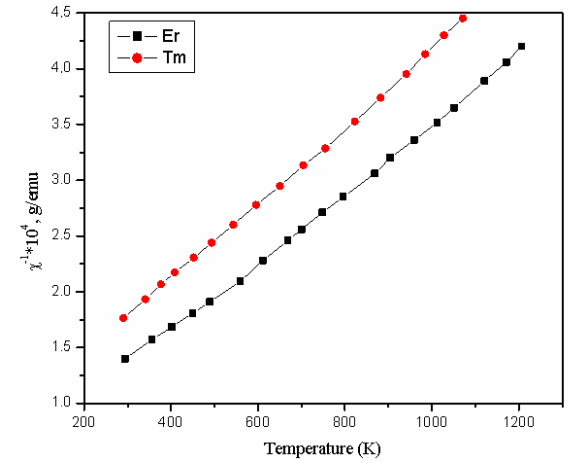

Fig. 8 Reciprocal magnetic susceptibility of the $ErCo_5Si_3$ and $TmCo_5Si_3$ compounds *vs.* temperature.

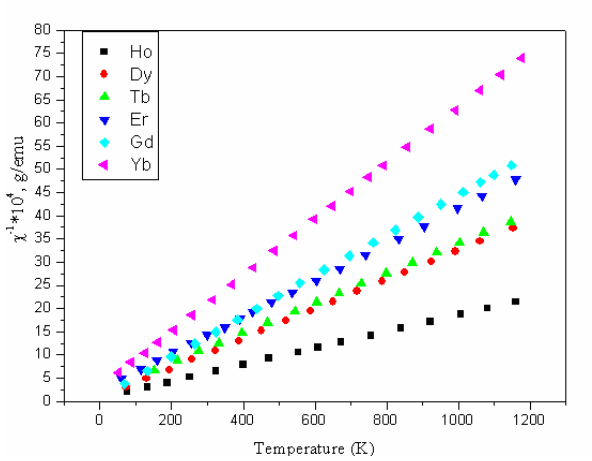

Fig. 9 Reciprocal magnetic susceptibility of the RNi_5Si_3 (R = Gd, Tb, Dy, Ho, Er, Yb) compounds *vs.* temperature.

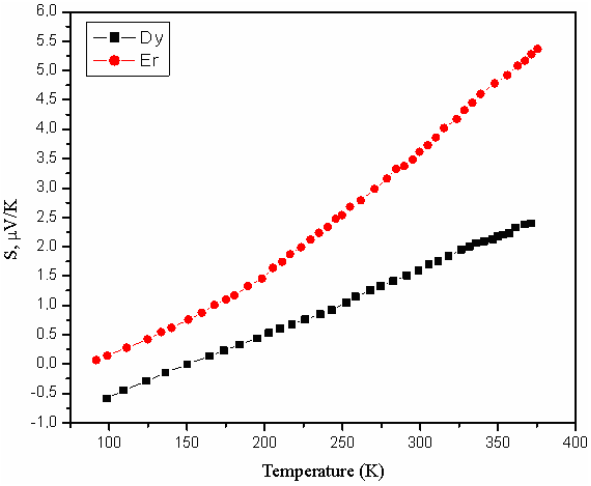

Fig. 10 Thermopower of the $DyCo_5Si_3$ and $HoCo_5Si_3$ compounds *vs.* temperature.

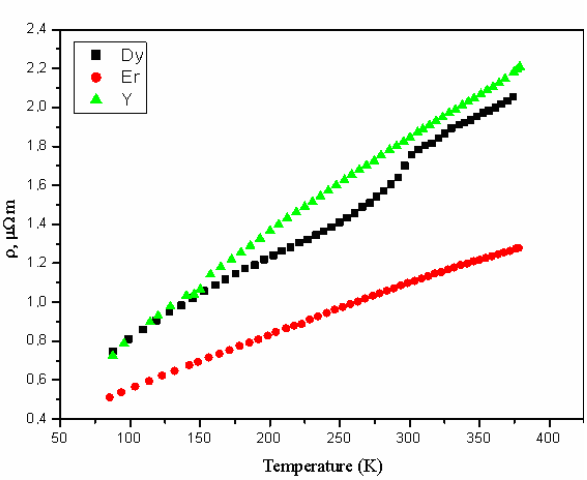

Fig. 11 Temperature dependence of the resistivity of the YCo_5Si_3, $DyCo_5Si_3$, and $ErCo_5Si_3$ compounds.

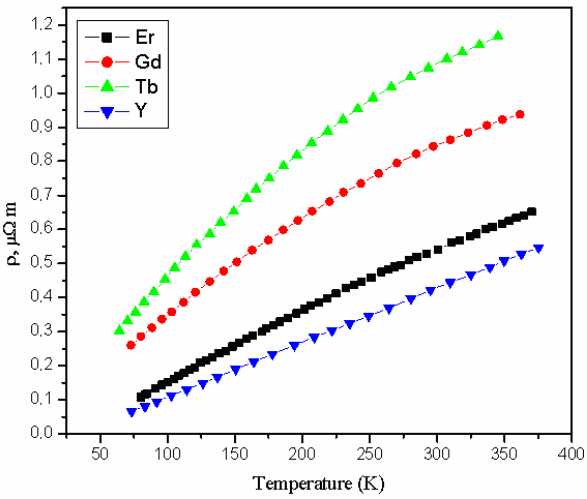

Fig. 12 Temperature dependence of the resistivity of the RNi_5Si_3 (R = Y, Gd, Tb, Er) compounds.

In the RCo_5Si_3 compounds the low-energy part, the $L_{II,III}$-band of silicon, is represented by a single maximum. The formation of a localized narrow 3*s*-band can be explained in the following way. In the crystal structure of RCo_5Si_3, the Si atoms are surrounded by Co or rare-earth element atoms, and therefore Si–Si direct contacts are practically not realized, which leads to strong localization of the 3*s*-like band.

The analysis of the parameters of the X-ray emission bands of cobalt (silicon) in the different RCo_5Si_3 compounds shows that the replacement of the rare-earth element weakly influences the structure of the valence band. It follows from the invariability of the peak intensities of the maxima D and E that the participation of *d*-states in the hybridization is similar. The ratio I_D/I_E for the RCo_5Si_3 compounds is somewhat larger than for the compounds with nickel.

It is possible to conclude from the aforesaid that an increase of the population of the 3*d*-levels of the transition metal weakens the hybridization ability of its *d*-states. This is in good agreement with conclusions based on calculations of the partial contributions to the intensity of the X-ray emission bands of the components for the composition RM_2Si_2 [12].

The decrease of the symmetry index of the Co $K\alpha$-line indicates a nonmagnetic state for the Co atoms. This occurs mainly at the cost of the low-energy part, so the line width is somewhat less, as compared with the same line for metallic cobalt. The change in the energetic parameters of the $K\alpha$-line of Co points to a decrease of the uncoupled spin density on the cobalt atoms, which explains the paramagnetism of cobalt in these intermetallics.

The conclusions based on the X-ray studies concerning the nonmagnetic state of the nickel and cobalt atoms in the RM_5Si_3 compounds were confirmed by an analysis of the magnetic characteristics of the compounds. The magnetic susceptibility of the YNi_5Si_3 compound is too small to classify this compound as a Pauli paramagnet. It decreases gradually from $0.61(1)\cdot10^{-6}$ emu·g^{-1} to $0.51(1)\cdot10^{-6}$ emu·g^{-1} in the temperature range 80÷295 K. The low field-independent susceptibility of $LuNi_5Si_3$ is also reduced from $0.86(1)\cdot10^{-6}$ at 80 K to $0.41(1)\cdot10^{-6}$ emu·g^{-1} at 295 K. We melted nine slightly non-stoichiometric compositions close to YCo_5Si_3 and found the minimum of susceptibility for the alloy $Y_{10.12}Co_{55.55}Si_{34.33}$ ($3.91\cdot10^{-6}$ emu·g^{-1} at 295 K). Therefore we have to presume that this enhanced Pauli susceptibility of the YCo_5Si_3 compound should be treated as a lack of magnetic moment on the Co atoms in the compound. Furthermore, the effective magnetic moments per f.u. presented in Table 1 (Figs. 8, 9) are fairly close to the corresponding calculated R^{3+} values. The behavior of the resistivity and the very low values of the thermopower in these compounds (Figs. 10, 11, 12) are typical for metallic materials.

Acknowledgements

The work was supported by the Ministry of Ukraine for Education and Science (grant 0109U002069).

References

[1] H.P.J. Wijn (Ed.), *Magnetic Properties of Metals*, Vol. III/32D, Springer-Verlag, Berlin Heidelberg, 2004, 407 p.
[2] V.I. Yarovets, *Ph.D. Thesis*, Lviv State University, 1978, 187 pp.
[3] Ya.P. Yarmolyuk, L.G. Aksel'rud, E.I. Gladyshevskii, *Kristallografiya* 23(5) (1978) 942.
[4] L.G. Aksel'rud, V.I. Yarovets, O.I. Bodak, Ya.P. Yarmolyuk, E.I. Gladyshevskii, *Kristallografiya* 21 (1976) 383.
[5] O. Bodak, Yu. Gorelenko, V. Yarovets, *Fiz. Khim. Tverd. Tila* 4(1) (2003) 401.
[6] *Oxford Diffraction, CrysAlis CCD, Version 1.170*, Oxford Diffraction Ltd., Abingdon, Oxford, England, 2004.
[7] *Oxford Diffraction, CrysAlis RED, Version 1.171*, Oxford Diffraction Ltd., Abingdon, Oxford, England, 2005.
[8] G.M. Sheldrick, *SHELXS97 and SHELXL97, WinGX Version, Release 97-2*, University of Göttingen, Germany, 1997.
[9] L.M. Gelato, E. Parthé, *J. Appl. Crystallogr.* 20 (1987) 139.
[10] L.G. Aksel'rud, Yu.N. Grin, P.Yu. Zavalii, V.S. Fundamensky, V.K. Pecharsky, *Universal Program Package for Single Crystal and/or Powder Structure Data Treatment, Coll. Abstr. XII Eur. Crystallogr. Meet.*, Moscow, 1989, Vol. 3, p. 155.
[11] Yu.K. Gorelenko, R.V. Skolozdra, I.D. Shcherba, V.I. Yarovets, *Neorg. Mater.* 29 (1993) 1638.
[12] O.I. Bodak, Yu.K. Gorelenko, V.I. Yarovets, I.D. Shcherba, G.A. Mel'nik, L.O. Dobryanska, R.V. Skolozdra, *Inorg. Mater.* 35 (1999) 360.
[13] I.D. Shcherba, V.M. Antonov, B.Ya. Kotur, *J. Alloys Compd.* 242 (1996) 58.
[14] R.V. Skolozdra, I.D. Shcherba, O.I. Bodak, G.A. Mel'nik, Yu.K. Gorelenko, V.I. Yarovets, L.O. Dobryanska, V.S. Lobojko, *J. Alloys Compd.* 296 (2000) 272.